

MHD simulations of polarized radio emission of adiabatic SNRs in ISM with nonuniform distribution of density and magnetic field

O.Petruk^{1,2}, R.Bandiera³, V.Beshley¹, S.Orlando², M.Miceli^{2,4}

¹Institute for Applied Problems in Mechanics and Mathematics (Lviv, Ukraine)

²INAF-Osservatorio Astronomico di Palermo (Italy)

³INAF-Osservatorio Astrofisico di Arcetri (Florence, Italy)

⁴Dipartimento di Fisica e Chimica, Università degli Studi di Palermo (Italy)

SNR images as diagnostic tools

A wealth of observational data on SNRs is available: fluxes, integral spectra, spatially-resolved *spectra*, *1D profiles* of brightness, *maps* of the surface brightness and of the *polarization* parameters etc. However, not all the data available are exploited. In particular, spectra, local features on the brightness maps – the radial (e.g. Ballet 2006) or azimuthal profiles (Fulbright, Reynolds 1990), contact discontinuity-shock separation (Warren et al. 2005) or protrusions (Rakowski et al. 2011), the rapidly varying spots (Uchiyama et al. 2007) or the ordered stripes (Eriksen et al. 2011) – attract attention while images of the overall SNR and polarization patterns are much less used.

In general, there are two ways to deal with SNR images: (a) to process the observed maps with minimal assumptions and (b) to model maps numerically starting from basic theoretical principles.

(a) With observed maps in different bands and with the only use of properties of emission processes, it is possible to separate the thermal and nonthermal X-ray images out of the mixed observed one (Miceli et al. 2009), to predict

gamma-ray images of SNRs (Petruk et al 2009a) or determine the magnetic field (MF) strength in the limbs of SNRs (Petruk et al. 2012).

(b) The method to simulate the synchrotron radio and X-ray images of spherical shell-like SNRs was developed and used for synchrotron maps by Reynolds (1998) and to gamma-ray images by Petruk et al. (2009b).

The simulation methodology was generalized to SNRs evolving in an ISM with *nonuniform* distributions of density and magnetic field: the asymmetries in the radio maps are studied by Orlando et al. (2007) and in X-rays and gamma-rays by Orlando et al. (2011).

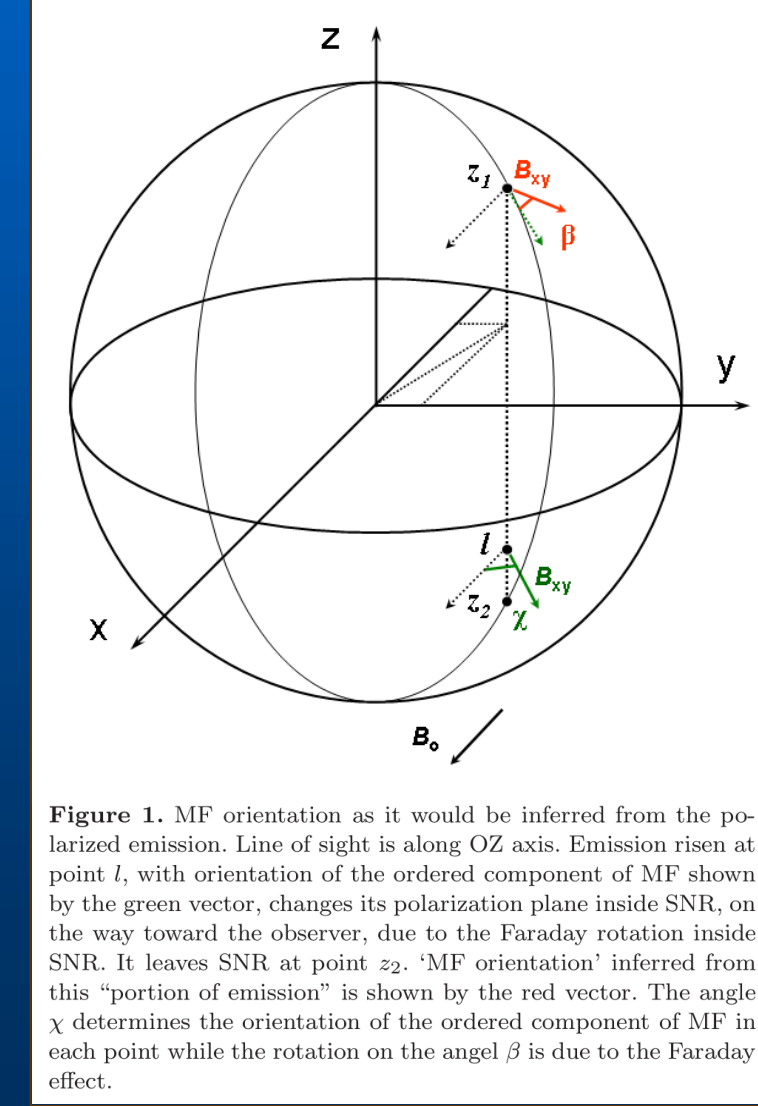
An approach to study the SNR *polarization* maps is presented in Bandiera & Petruk (2016).

Here, we report the further development of the approach (b). Namely, the method to model *maps of the Stokes parameters for the shell-like adiabatic SNRs* is presented together with related MHD simulations, including *nonuniform ISM conditions*.

Modeling the SNR polarization maps

Model components:

- 3-D MHD structure of SNR
- evolution of cosmic rays (CRs) around the shock and downstream
- evolution and 3-D structure of the *turbulent MF* component, considering its interaction with CRs
- calculation of *polarized emission* in each point inside the SNR (Stokes parameters)
- projection on the plane of the sky
 - including *internal Faraday rotation*
 - for a given *orientation* of SNR and ambient MF with respect to the observer
 - for *uniform and nonuniform ISM / interstellar MF*



In each point, the Stokes parameters, in the laboratory frame, are

$$\begin{cases} I = I' \\ Q = Q' \cos 2\chi + U' \sin 2\chi = Q' \cos 2\chi \\ U = -Q' \sin 2\chi + U' \cos 2\chi = -Q' \sin 2\chi \\ V = V' = 0 \end{cases}$$

where the primed values are in the local frame (where $U=0$),

$$\begin{cases} \cos 2\chi = \frac{B_x^2 - B_y^2}{B_x^2 + B_y^2} \\ \sin 2\chi = \frac{2B_x B_y}{B_x^2 + B_y^2} \end{cases}$$

$$\beta(z_1, z_2) = \frac{e^3 \lambda^2}{2\pi m_e^2 c^4} \int_{z_1}^{z_2} n(z') B_z(z') dz'$$

The projected Stokes parameters are

$$\begin{cases} I = \int_{z_1}^{z_2} I' dl \\ Q = \int_{z_1}^{z_2} Q' \cos 2(\chi + \beta) dl \\ U = \int_{z_1}^{z_2} Q' \sin 2(\chi + \beta) dl \end{cases}$$

Emissivity in ordered + disordered field

• The classical synchrotron emission theory is developed for the ordered MF (uniform on the scale $\gg r_L$ where r_L is the Larmor radius).

• However, if the model considers the only ordered MF, then Π is maximum, 0.69 for $s=2$. Observations reveal on average $\Pi \sim 15\%$ (with local maxima around 35-50%; Reynoso et al. 2013). Therefore, the presence of a disordered component of MF is necessary.

At this point, we face the following two problems: we need

✓ An extension of the classical theory of synchrotron emission

to ordered + disordered MF

✓ A description of structure of *turbulent MF* component in SNR

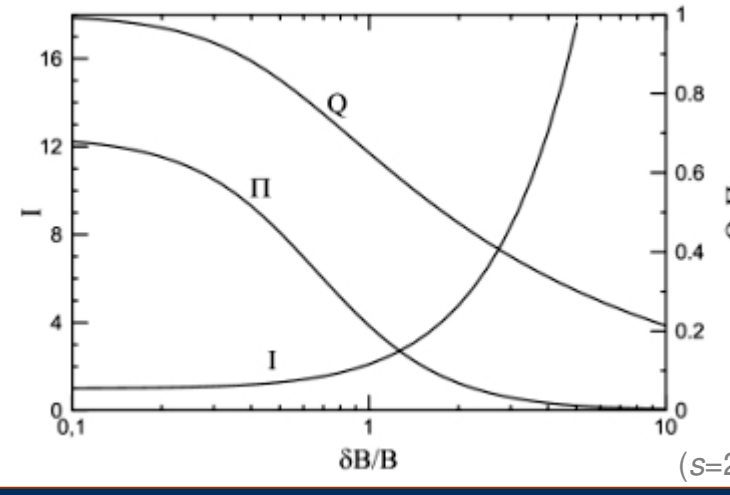
If the particles with the power-law momentum distribution emit in MF which has ordered component of the strength B and the random component represented by the spherical Gaussian with the standard deviation δB then the Stokes parameters are

$$\begin{aligned} I' &= I_0 \left\{ 2^{(s+1)/4} \Gamma \left(\frac{s+5}{4} \right) \left(\frac{\delta B}{B} \right)^{(s+1)/2} {}_1F_1 \left(-\frac{1+s}{4}, 1, -\frac{1}{2} \left(\frac{\delta B}{B} \right)^{-2} \right) \right\}; \\ Q' &= Q_0 \left\{ 2^{(s-7)/4} \Gamma \left(\frac{s+9}{4} \right) \left(\frac{\delta B}{B} \right)^{(s-3)/2} {}_1F_1 \left(\frac{3-s}{4}, 3, -\frac{1}{2} \left(\frac{\delta B}{B} \right)^{-2} \right) \right\}, \end{aligned}$$

where ${}_1F_1(a, b, z)$ is the Kummer confluent hypergeometric function, I_0 and Q_0 are respective Stokes parameters for the case of the ordered MF.

Note, that I increases with $\delta B/B$. This is of importance for fitting the observed synchrotron spectra. In particular, if one assumes $\delta B/B \sim 1$ then the flux is twice the flux given by the classic synchrotron theory.

Fig. The ratios: I'/I_0 , Q'/Q_0 , Π/Π_0



[for details see Poster S1.2 and Bandiera & Petruk 2016]

Turbulent magnetic field component

I' , Q' depend on $\delta B/B$. Need to know it in each point inside the SNR.

Equation for the wave evolution is [McKenzie & Völk 1982]

$$\frac{\partial P_w}{\partial t} + u \frac{\partial P_w}{\partial r} + P_w \frac{3}{2} \frac{\partial u}{\partial r} = \frac{1}{2} (\sigma_w P_w - \Gamma_w P_w)$$

$$P_w = \delta B^2 / 8\pi$$

growth [Amato & Blasi 2006]

$$\sigma_w P_w = \left| v_A \cos \Theta \right| \frac{\partial P_w}{\partial r}$$

damping [Ptuskin & Zirakashvili 2003]

$$\Gamma_{NL} P_w = \frac{2 c k v_A \cos \Theta}{B^2 / 8\pi} k_{min} P_w^2$$

Re-written in the Lagrangian coordinate a

$$\left(\frac{\partial}{\partial t} + u \frac{\partial}{\partial r} \right)_E = \left(\frac{d}{dt} \right)_L, \quad \left(\frac{\partial}{\partial r} \right)_E = \frac{\rho(a) r(a)^2}{\rho_0(a) a^2} \left(\frac{\partial}{\partial a} \right)_L$$

it is the Riccati differential equation

$$\frac{dP_w(a, t)}{dt} + q_1(a, t) P_w(a, t) + q_2(a, t) P_w(a, t)^2 = q_0(a, t)$$

with

$$q_0 = \frac{v_A \cos \Theta}{2 \rho_0 a^2} \frac{\partial P_w}{\partial a}$$

$$q_1 = \frac{3 \rho^2}{2 \rho_0 a^2} \frac{\partial u}{\partial a}$$

$$q_2 = \frac{c k v_A \cos \Theta}{B^2 / 8\pi} k_{min}$$

$$\delta B(a, t) = \sqrt{8\pi P_w(a, t)}$$

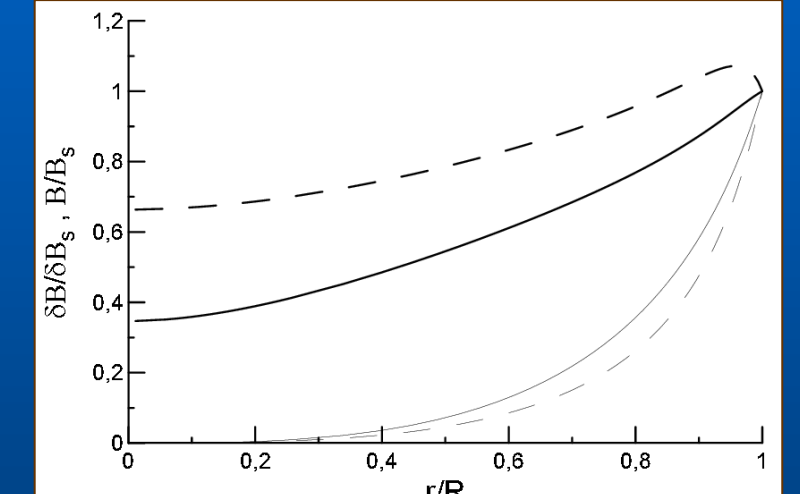


Fig. Normalized radial profiles of $B(r)/B_s$ (thin lines) and $\delta B(r)/\delta B_s$ (thick lines) downstream of the parallel Sedov shock (solid lines) and the perpendicular shock (dashed lines).

- Alfvén waves are considered
- interactions with CRs are accounted

- The ratio $\delta B/B$, being <1 at the shock, increases toward the center of the SNR
- The normalized δB is larger for a perpendicular shock compared to a parallel shock **but** the physical one is smaller because δB is proportional to $(\cos \Theta)^{1/2}$.

SNR in uniform medium

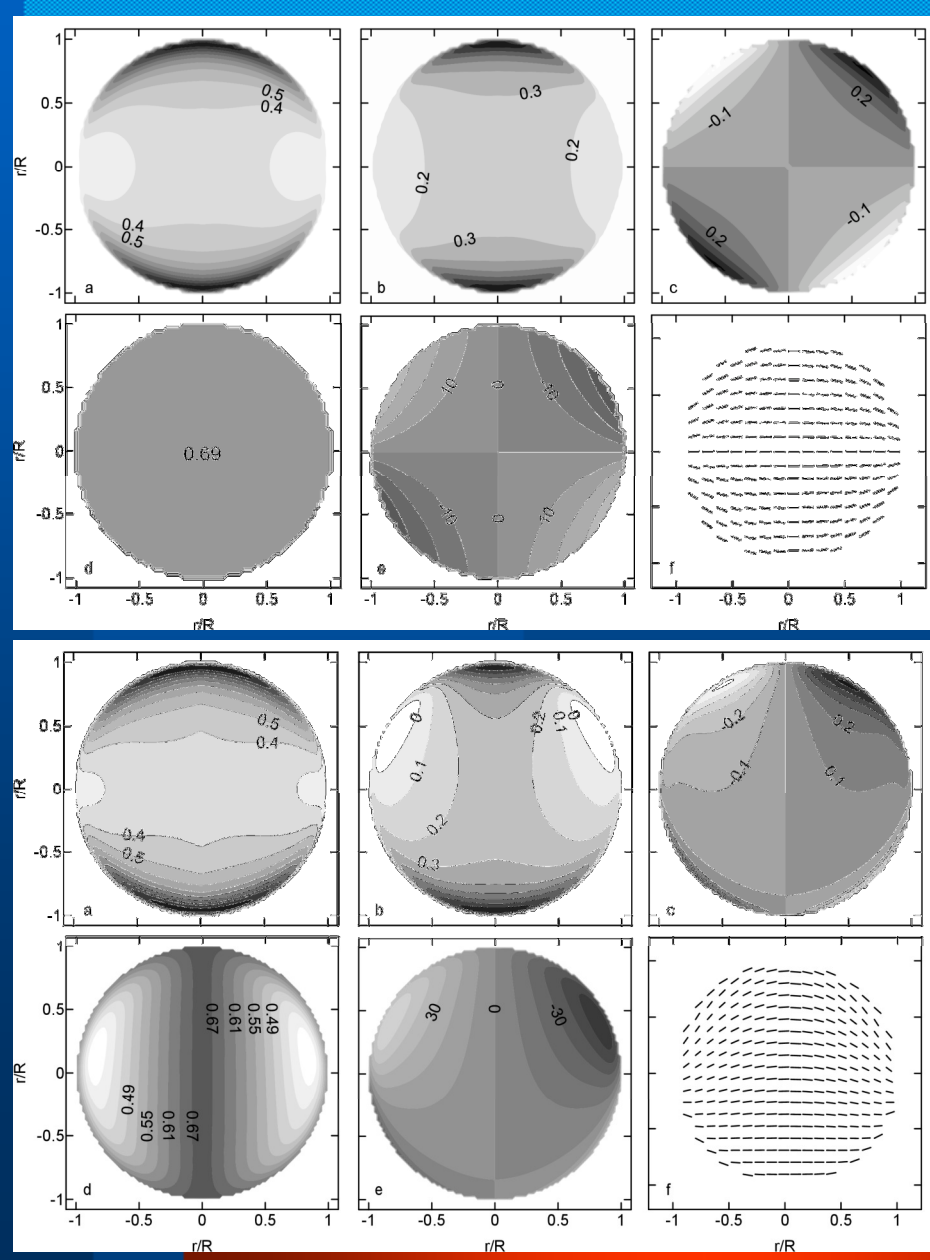


Fig. A: Reference model. I , Q , U , Π , angle of MF Ψ and MF map. No turbulent MF, no internal Faraday rotation (isotropic injection; $(\delta B/B)=0.3$)

Fig. B: The same as Fig. A with • *turbulent MF* and • *internal Faraday rotation*.

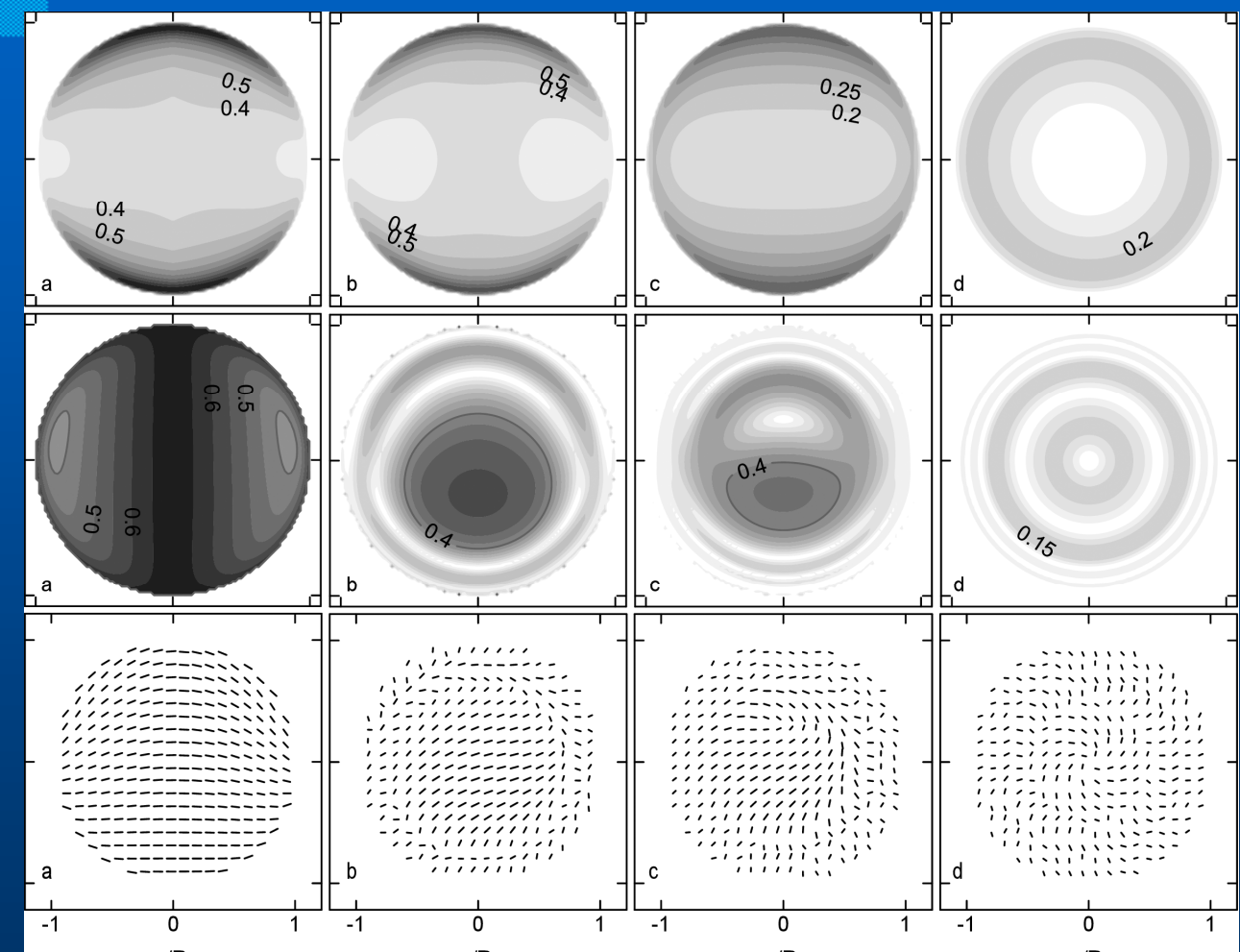


Fig. C: I , Π and MF map for different aspect angle (between MF and LoS): 90° (a), 60° (b), 30° (c), 0° (d). MF vectors are proportional to Π .

ISM density gradient

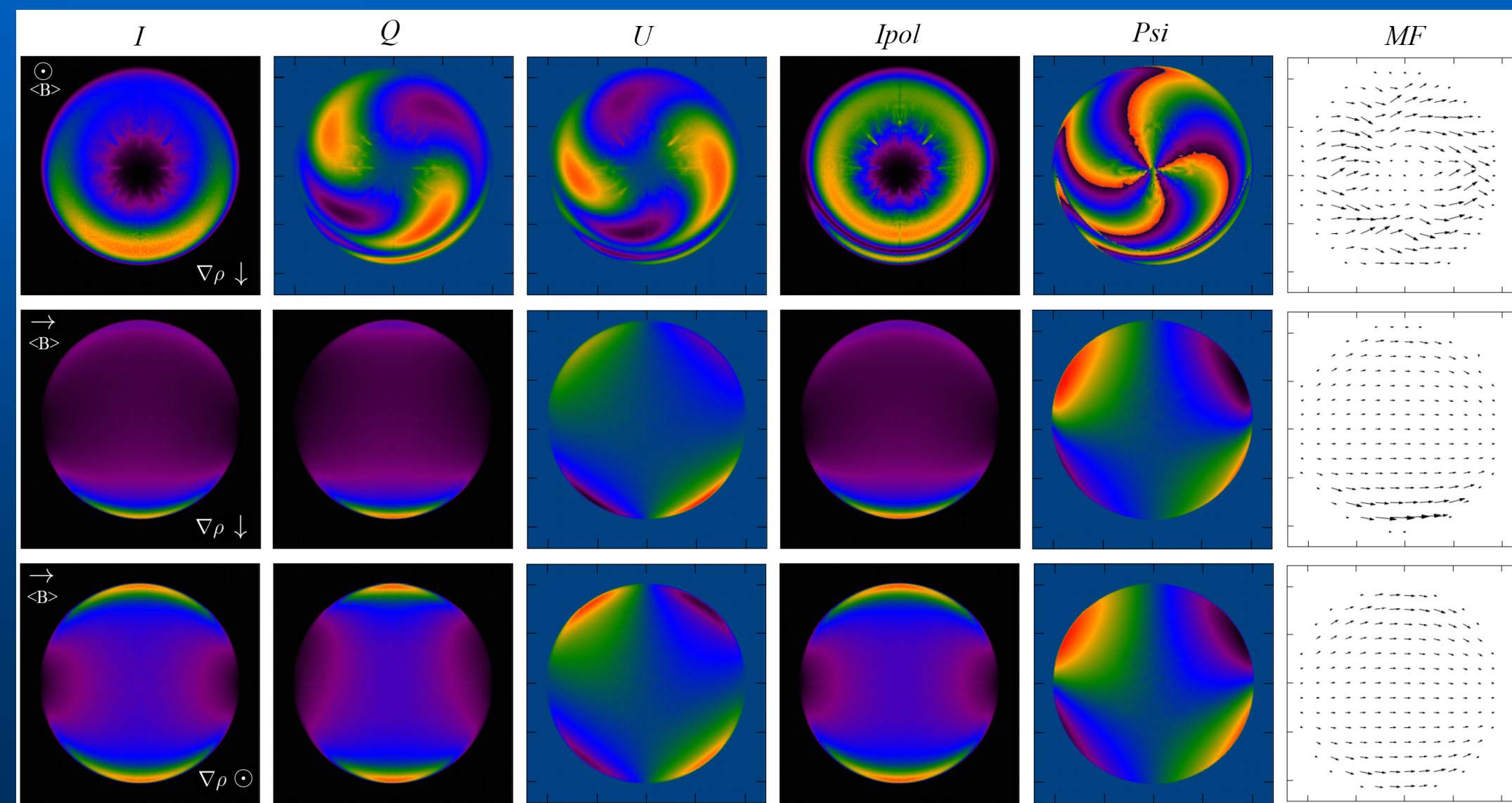


Fig. D: Full three-dimensional MHD simulations of SNR in ISM with density gradient (with the use of FLASH code: Fryxell et al. 2000). View from different orientations. quasiperpendicular injection, isotropic injection case is quite similar (Ipol – polarized intensity, Psi – is the MF angle) Details of the numerical realization and CR description in the nonuniform medium are presented in Orlando et al. (2007).

Ambient magnetic field gradient

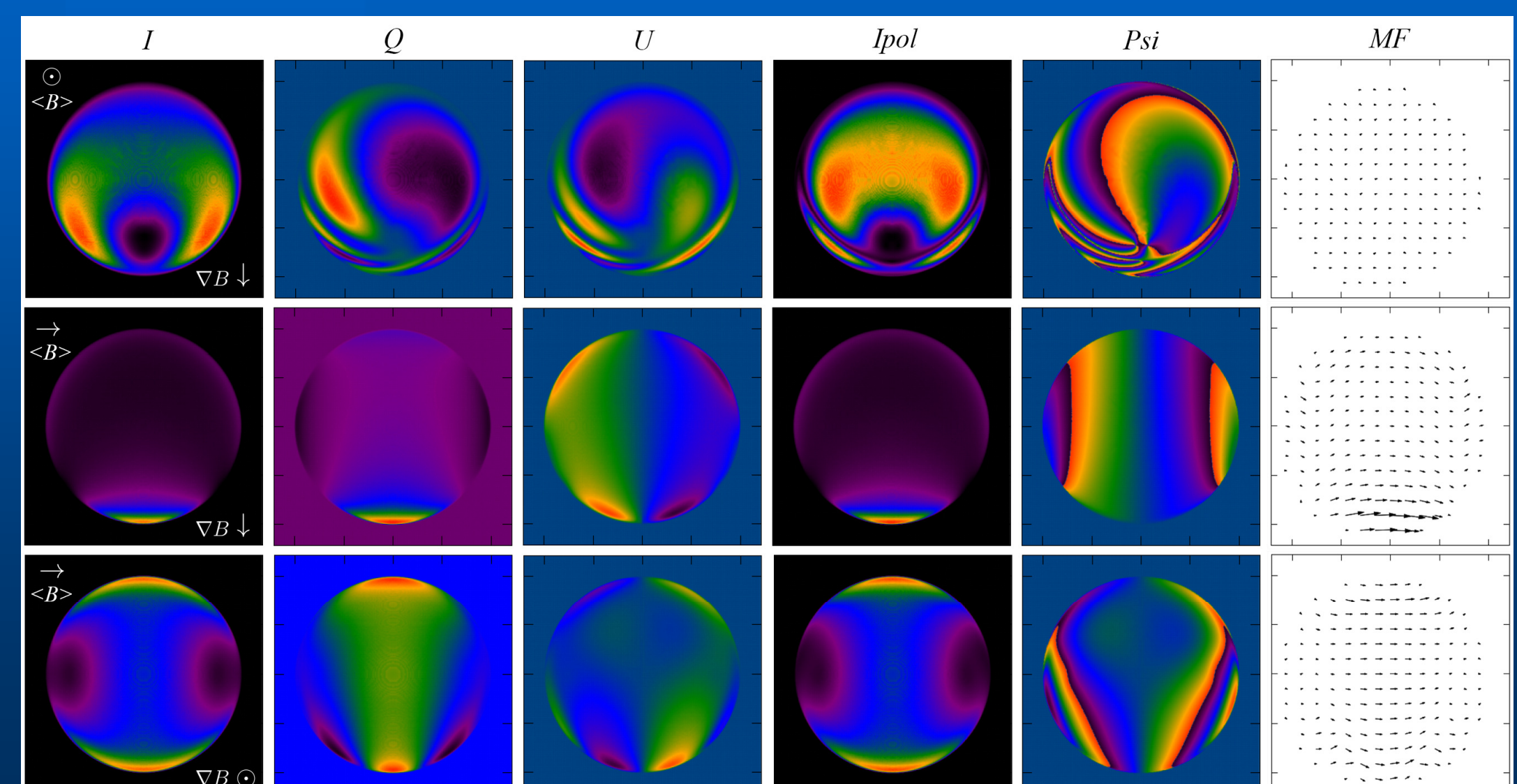


Fig. E: Full three-dimensional MHD simulations of SNR in ISM with gradient of MF (with FLASH code). View from different orientations. quasiperpendicular injection, isotropic injection case is quite similar MF vectors are proportional to Ipol.

Details of the numerical realization and CR description in the nonuniform medium are presented in Orlando et al. (2007).

Conclusions and References

- A method to model polarization images of adiabatic SNRs is developed which includes a generalization of the synchrotron emission theory to ordered+random MF and a description of the turbulent field inside a SNR
- The flux depends on the ratio $\delta B/B$, e.g., if $\delta B/B=1$ it is twice the flux in the only ordered field
- A turbulent component of the MF lowers the polarization fraction: the larger $\delta B/B$ the smaller the fraction
- The Faraday effect in the SNR interior is important in formation of SNR polarization patterns
- *grad B* and / or *grad rho* affect SNR images as well
- The surface brightness distributions are similar if either a *grad rho* or a *grad B* is present in ISM. The polarization patterns could help to distinguish between the two cases

Acknowledgements. The MHD simulations were executed at CINECA (Bologna, Italy) with the software in part developed by ASC/Alliance Center for Astrophysical Thermonuclear Flashes at the University of Chicago. The polarized emission simulations were performed on the computational cluster at IAPMM (grant 0115U002936). This work is partially funded by the PRIN INAF 2014 grant.

Ballet 2006 *Adv. Space Res.* 37, 1902
Bandiera, Petruk 2016 *MNRAS* 459, 178
Eriksen et al. 2011 *ApJ* 728, L28
Fryxell et al. 2000 *ApJS* 131, 273
Fulbright, Reynolds 1990 *ApJ* 357, 591
Miceli et al. 2009 *A&A* 501, 239
Orlando et al. 2007 *A&A* 470, 927
Orlando et al. 2011 *A&A* 526, A129
Petruk et al. 2009a *MNRAS* 399, 157
Petruk et al. 2009b *MNRAS* 395, 1467
Petruk et al. 2012 *MNRAS* 419, 608
Rakowski et al. 2011 *ApJ* 735, L21
Reynolds 1998 *ApJ* 493, 375
Reynoso et al. 2013 *AJ* 145, 104
Uchiyama et al. 2007 *Nature* 449, 576
Warren et al. 2005 634, 376